

Fig. 3 Radial variation of total pressure P at $L/L_0 = 0.43$. To make these curves comparable to those in Fig. 2, the propeller support was placed in the chamber in order to produce comparable obstruction to flow. The curve marked "no obstruction" shows that the pressure distribution remained similar without obstruction.

The flow direction was measured by means of a hinged flag. By orienting the hinge axis in two mutually perpendicular directions (e.g., parallel and perpendicular to the chamber axis) and observing the flag positions, it was possible to determine the flow direction as the intersection of the two flag planes, except for some corrections that must be applied to account for the effect of radial pressure gradients in the flow field. At the walls, the flow directions were determined from the streaking marks.

The total pressure was measured by means of a pitot tube in the conventional manner.

The flow data obtained this way were checked against the mass rate of flow, which was also measured. The agreement was satisfactory.

Results and Discussion

Figures 2 and 3 show typical results of the rotational speed and total pressure measurements, respectively. In Fig. 2, the qualitative agreement of the V_ϕ vs D/D_0 curve with similar curves computed for the vortex tube, by Suzuki,² for example, is evident. The main result, however, was that the flow profile elsewhere in the chamber (except in the boundary layers near the solid walls) remained essentially the same as in these figures. This result was not altered by shortening the chamber length by a factor of three or by stopping one of the central holes in the end plate. Thus, in the range of variables investigated here, the flow field in the interior of the chamber had the characteristics of a strong two-dimensional vortex superimposed on a weak sink at the center. No important secondary flow³ was observed. Of special interest was the falling pressure toward the chamber axis (Fig. 3) and the accompanying radial flow inward along the entire axis. It is conjectured that these features have a strong stabilizing influence on the arc column along the axis when such a chamber is used as a plasmajet generator.

References

- 1 Pfender, E., "Generation of an almost fully ionized, spectrally clean, high density hydrogen plasma," *Proceedings of the 6th*

International Conference on Ionization Phenomena in Gases, edited by P. Hubert and E. Crémieu-Alcan (Paris, 1963), Vol. II, pp. 369-374.

² Suzuki, M., "Theoretical and experimental studies on the vortex tube," *Sci. Papers Inst. Phys. Chem. Res. (Tokyo)* **54**, 43-87 (1960).

³ Rosenzweig, M. L., Ross, D. H., and Lewellen, W. S., "On secondary flows in jet driven vortex tubes," *J. Aerospace Sci.* **29**, 1142 (September 1962).

Pressure Variation in a Tank Undergoing an Acceleration

R. C. PROGELHOF*

Lehigh University, Bethlehem, Pa.

Nomenclature

- a = speed of sound
- L = length
- p = pressure
- t = time
- u = magnitude of flow velocity
- x = distance
- α = acceleration
- γ = ratio of specific heats
- τ = nondimensional time

Subscript

- 0 = initial conditions

Introduction

IN a recent technical note by Ehlers,¹ a solution was presented for the linearized equations of motion for the one-dimensional homentropic flow of a perfect gas in a cylindrical vessel of uniform cross-sectional area undergoing a unit constant acceleration in the direction of the major axis of the vessel. However, it is not necessary to linearize the equations of motion in order to obtain the pressure distribution in the vessel as a function of time, but a numerical or graphical technique based on the method of characteristics can be readily used. This note outlines the graphical technique that was used to obtain the pressure variation in the vessel as a function of time for two acceleration rates that are constant with time. From the pressure-time results obtained from the method of characteristics, an estimate can be made as to the maximum nondimensional acceleration for which the linearized approach can be used to approximate the pressure distribution in the vessel.

Theory

The four quasilinear equations of motion are the continuity equation (1), momentum equation (2), and Eqs. (3) and (4), relating the independent variables x and t and dependent variables a and u with four unknown partial derivatives^{3,4}:

$$a \frac{\partial u}{\partial x} + \frac{2}{\gamma - 1} \frac{\partial a}{\partial t} + \frac{2u}{\gamma - 1} \frac{\partial a}{\partial x} = 0 \quad (1)$$

$$\frac{\partial u}{\partial t} + u \frac{\partial u}{\partial x} + \frac{2a}{\gamma - 1} \frac{\partial a}{\partial x} = \alpha(t) \quad (2)$$

$$\frac{\partial u}{\partial t} dt + \frac{\partial u}{\partial x} dx = du \quad (3)$$

$$\frac{\partial a}{\partial t} dt + \frac{\partial a}{\partial x} dx = da \quad (4)$$

Received April 23, 1964.

* Assistant Professor, Department of Mechanical Engineering. Member AIAA.

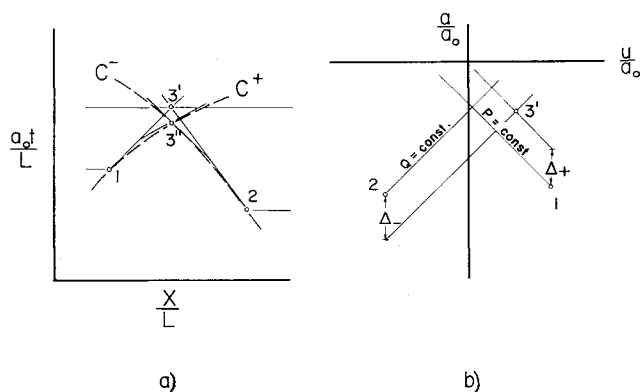


Fig. 1 Graphical technique: a) physical plane, b) state plane.

Applying Cramer's rule to the foregoing set of equations, the unknown partial derivatives $\partial u/\partial t$, $\partial u/\partial x$, $\partial a/\partial t$, and $\partial a/\partial x$ will be the ratio of two determinants:

$$\frac{\partial u}{\partial t} = \frac{K_1}{N}, \quad \frac{\partial u}{\partial x} = \frac{K_2}{N}, \quad \frac{\partial a}{\partial t} = \frac{K_3}{N}, \quad \frac{\partial a}{\partial x} = \frac{K_4}{N}$$

A characteristic line is defined as a line in space on which the derivatives of the flow properties are indeterminate and thus may undergo a discontinuity. The derivatives only can be indeterminate if the determinants N_1 , K_1 , K_2 , K_3 , and K_4 are set identically equal to zero:

$$N = \begin{vmatrix} 0 & a & \frac{2}{\gamma-1} & \frac{2u}{\gamma-1} \\ 1 & u & 0 & \frac{2a}{\gamma-1} \\ dt & dx & 0 & 0 \\ 0 & 0 & dt & dx \end{vmatrix} = 0$$

and, expanding,

$$dx/dt = u \pm a \quad (5)$$

The curve in the $x-t$ plane for which $dx/dt = u + a$ is denoted as a C^+ physical characteristic and similarly $dx/dt = u - a$ as a C^- physical characteristic. Setting the determinant K_1 equal to zero,

$$\begin{vmatrix} 0 & a & \frac{2}{\gamma-1} & \frac{2u}{\gamma-1} \\ \alpha(t) & u & 0 & \frac{2a}{\gamma-1} \\ du & dx & 0 & 0 \\ da & 0 & dt & dx \end{vmatrix} = 0$$

and expanding,

$$\pm \frac{du}{dt} + \frac{2}{\gamma-1} \frac{da}{dt} = \pm \alpha(t) \quad (6)$$

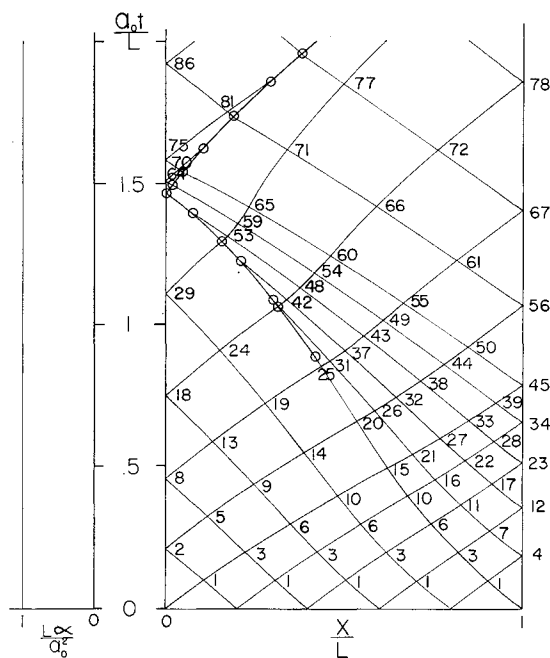
The plus sign corresponds to the determinant being evaluated along a C^+ characteristic and the minus sign along a C^- physical characteristic. Equation (6) is a compatibility equation relating the flow properties u and a along a physical characteristic. Evaluating the determinants K_2 , K_3 , and K_4 will produce redundant information. To simplify the graphical technique, Eqs. (5) and (6) are rewritten in de Haller² nondimensional notation:

$$\frac{d(x/L)}{d\tau} = \frac{u}{a_0} \pm \frac{a}{a_0} \quad (7)$$

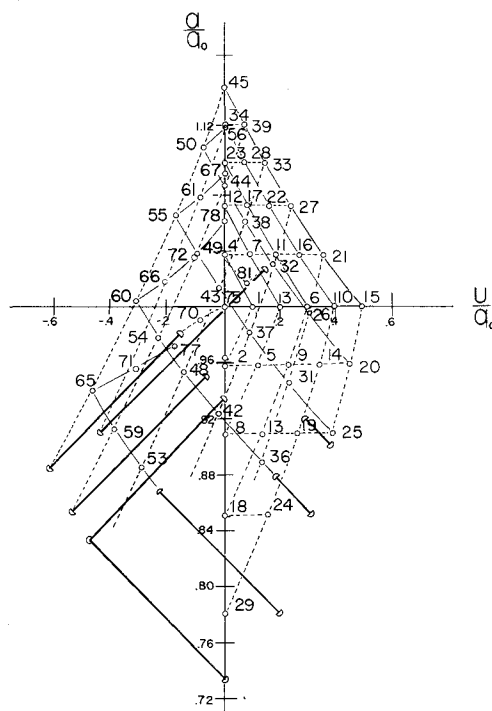
$$\frac{d \{ [2/(\gamma-1)] (a/a_0) \pm (u/a_0) \}}{d\tau} = \pm \frac{L\alpha}{a_0^2} \quad (8)$$

where $\tau = a_0 t/L$.

Equations (7) and (8) represent the starting point of the graphical solutions. To illustrate the graphical method of obtaining a solution, assume that two points, 1 and 2, are known in the $x-t$ plane, commonly referred to as the physical plane, and their corresponding position is fixed in the $a-u$ plane, referred to as the state plane (see Fig. 1). Point 3, the point that we are trying to find, lies on the intersection of the C^+ and C^- characteristics. The first estimate of point 3 in the physical plane, point 3', is fixed by the intersection of the



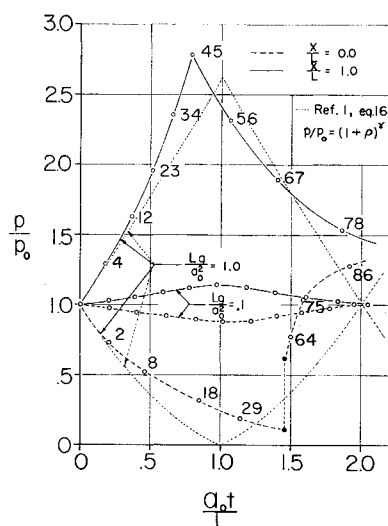
a) Physical plane



b) State plane

Fig. 2 Graphical solution for a unit constant nondimensionalized acceleration.

Fig. 3 Pressure vs nondimensionalized time.



slopes of the C^+ and C^- characteristics evaluated at points 1 and 2, respectively. The values of τ_{23}' and τ_{13}' are read directly from the physical plane (Fig. 1a). If we denote

$$\frac{2}{\gamma - 1} \frac{a}{a_0} + \frac{u}{a_0} = P$$

$$\frac{2}{\gamma - 1} \frac{a}{a_0} - \frac{u}{a_0} = Q$$

their graphic representations are straight lines in the state plane (Fig. 1b). Hence, Eq. (8) represents the change in the variables P and Q with respect to time; thus,

$$P_3 = P_1 + (\delta P / \delta \tau) \Delta \tau_{13} = P_1 + (L\alpha / a_0^2) |_{av} \Delta \tau_{13}$$

$$Q_3 = Q_2 + (\delta Q / \delta \tau) \Delta \tau_{23} = Q_2 - (L\alpha / a_0^2) |_{av} \Delta \tau_{23}$$

Since the value of $L\alpha / a_0^2$ is fixed, the first estimates of $P_3 - P_1 = \Delta_+$ and $Q_3 - Q_2 = \Delta_-$ can be made and point 3' fixed in the state plane. A new estimate of point 3 is made in the physical plane, point 3'', and the iteration process continued until the values converge on point 3. The boundary condition that must be satisfied during the construction of the solution in the state and physical is that the gas velocity at both ends of the vessel must be zero.

The advantage of the graphical approach is that problems with very difficult boundary conditions can be solved with the same ease as the examples presented, whereas it may be very difficult if not impossible to obtain the inverse transform for the linearized equations of motion and apply the boundary conditions.

Two solutions have been carried out for a unit constant nondimensionalized acceleration, $L\alpha / a_0^2$, of 1 and 0.1 for a comparison with the linearized approach. The state and physical planes are only shown for the larger value of acceleration (Fig. 2). From the isentropic relationship of pressure vs speed of sound, the pressure variation at each end of the vessel is plotted in Fig. 3.

Analysis of Results

From Fig. 3, it is clearly seen that the pressure deviates significantly from the reference or initial value for the largest nondimensionalized acceleration. In addition, the pressure waves do not appear as simple harmonics, as would be expected from the linearized approach. A shock wave with a pressure ratio of about 2.4 is formed inside the vessel. At the lower acceleration rate, the deviations are much smaller; however, a definite shift of pressure vs time curve due to the nonlinearity of the equations of motion is still noticeable.

Conclusion

The pressure-time history due to the motion of a perfect gas in a cylindrical vessel of uniform cross-sectional area

undergoing an arbitrary acceleration as a function of time in the direction of the major axis of the vessel can be obtained through the application of a graphical or numerical technique based on the method of characteristics. A comparison of the pressure-time curves for the system undergoing a unit constant acceleration indicates that the results based on linearizing the equations of motion¹ will be in close agreement with those based on the method of characteristics for a nondimensionalized acceleration, $L\alpha / a_0^2$, less than 0.1.

References

- ¹ Ehlers, F. E., "Linearized analysis of the pressure waves in a tank undergoing an acceleration," *AIAA J.* **2**, 110-112 (1964).
- ² deHaller, P., "On a graphical method of gas dynamics," *Sulzer Tech. Rev. Switz.* **1**, 6-24 (1954).
- ³ Rudinger, G., *Wave Diagrams for Nonsteady Flow in Ducts* (D. Van Nostrand Co., Inc., New York, 1955), Chaps. 3-5.
- ⁴ Shapiro, A., *The Dynamics on Thermodynamics of Compressible Fluid Flow* (Ronald Press Co., New York, 1953), Vols. 1 and 2, Chap. 24.

Quadratic Effects of Frequency on Aerodynamic Derivatives

KAZIMIERZ J. ORLIK-RÜCKEMANN*
National Aeronautical Establishment,
Ottawa, Ontario, Canada

STATIC and dynamic stability derivatives determined from oscillatory experiments in wind tunnels often display significant effects of reduced frequency. Although it is common practice to present such effects in graphical form, it is suggested here that often it may be preferable to use an analytical presentation, involving second- and third-order derivatives. The analysis of the equation of motion for a single-degree-of-freedom oscillatory system is presented here with emphasis on the effect of these additional derivatives in the general case of amplitude that varies with time. This new approach is illustrated with some examples, based on a recent wind-tunnel investigation of sweptback wings at supersonic speeds.

Equation of Motion

The following expressions are given in terms of variables and coefficients applicable to an oscillatory motion in pitch but, of course, can be adapted for any single-degree-of-freedom oscillation. The equation of motion for such a system can be written as

$$I\ddot{\theta} + \gamma\dot{\theta} + K\theta = M \quad (1)$$

where I is moment of inertia, γ is mechanical damping coefficient, K is mechanical stiffness coefficient, and θ , $\dot{\theta}$, and $\ddot{\theta}$ are the angle of oscillation in pitch around a fixed axis† and its first and second derivatives with respect to time, respectively. M is the aerodynamic pitching moment, which, in turn, can be expressed in terms of successive time derivatives of the angle of oscillation, viz.,

$$M = M_\theta\theta + M_{\dot{\theta}}\dot{\theta} + M_{\ddot{\theta}}\ddot{\theta} + M_{\ddot{\theta}}\ddot{\theta} + \dots \quad (2)$$

where $\ddot{\theta}$ is the third time derivative of the angle of oscillation, and M_θ , $M_{\dot{\theta}}$, $M_{\ddot{\theta}}$, and $M_{\ddot{\theta}}$ are the successive pitching moment derivatives.‡

Received May 7, 1964; revision received June 15, 1964.

* Head, Unsteady Aerodynamics Laboratory. Associate Fellow Member AIAA.

† Thus, compared to standard nomenclature, we have $M_\theta = M_\alpha$ but $M_{\dot{\theta}} = M_q + M_{\dot{\alpha}}$.

‡ The second- and third-order derivatives are denoted by $M_{\ddot{\theta}}$ and $M_{\ddot{\theta}}$ to avoid double and triple dotted subscripts.